

Dynamic Range of Frequency Modulated Direct-Detection Analog Fiber Optic Links

John M. Wyrwas, *Student Member, IEEE*, and Ming C. Wu, *Fellow, IEEE*

Abstract—A frequency modulated (FM) analog optical link using an FM discriminator is analyzed. Figures-of-merit are derived, including expressions for the second-order (OIP2) and third-order intercept points (OIP3), spurious-free dynamic range (SFDR) and noise figure (NF). It is found that a discriminator with linear field transmission and constant group delay will produce no third-order or higher-order distortions, and balanced detection will suppress the remaining second-order distortion. Low biasing the discriminator is found not to improve the NF of the link. Residual intensity modulation (IM) of the laser is shown to significantly increase the link's distortion. A discriminator using tenth-order finite-impulse response (FIR) filters implemented in planar lightwave circuits (PLC) is proposed and shown to improve OIP3 by 31 dB over a Mach-Zehnder interferometer (MZI) discriminator.

Index Terms—Frequency discriminator, microwave-photonic link, optical frequency modulation, optical link, radio-over-fiber.

I. INTRODUCTION

ANALOG fiber optic links have been explored for applications in antenna remoting, cable television, phased array radar and cellular communication links because of advantages in size, weight, immunity to electromagnetic interference, bandwidth and power over traditional coaxial links [1]–[3]. The most common analog fiber optic links use intensity modulation (IM) where the optical power is varied in proportion to the input signal. The dynamic ranges of these links suffer from relative intensity noise (RIN) and third-order intermodulation distortion (IMD) [4].

Frequency modulated (FM) links, where the optical frequency of the laser is varied with the input signal, are considered as promising alternatives to IM links. Carrier relaxation processes do not limit the bandwidth of a directly modulated FM laser [5]. High FM purity [6] and modulation efficiency [7] are possible.

A coherent detection system using optical heterodyning is often used to recover FM [8] but adds undesired complexity at the receiver. To avoid optical heterodyning, many authors have studied FM direct-detection (FM-DD) links. In an FM-DD link, an optical filter acts as an FM discriminator that converts FM to IM before the photodetector [9].

Manuscript received May 21, 2009; revised August 24, 2009. First published September 09, 2009; current version published November 11, 2009. This work was supported in part by the National Science Foundation through CIAN NSF ERC under Grant EEC-0812072.

The authors are with the Department of Electrical Engineering and Computer Sciences, University of California at Berkeley, CA 94720-1770 USA (e-mail: jwyrwas@eecs.berkeley.edu; wu@eecs.berkeley.edu).

Digital Object Identifier 10.1109/JLT.2009.2031986

Mach-Zehnder interferometers (MZI) were first suggested as FM discriminators [10]–[12], but suffer from large third-order distortion. Alternatives to MZIs have been proposed, including fiber Bragg gratings (FBGs) [13]–[18] and interferometers linearized with ring resonators [19], [20]. Each filter's optical intensity transmission ramps linearly with frequency, which is a signature of incoherent optical signal processing [21]. Because of long coherence lengths of lasers used in communication systems, practical integrated filters, such as those implemented in planar lightwave circuits (PLCs), are coherent and are appropriately analyzed as a function of electric field transmission. The MZI itself filters coherently. If the optical filtering is coherent, we find that a linear intensity ramp is not a distortion-less discriminator.

In this paper, we derive figures-of-merit for an FM-DD link that uses an arbitrary filter. Using a two-tone test, we find small-modulation-depth approximations for the current at each microwave frequency. We obtain equations for the signal-to-noise ratio (SNR), second-order and third-order output intercept points (OIP2 and OIP3), spurious-free dynamic range (SFDR) and noise figure (NF). We find that a filter that has linear phase and whose electric field transmission ramps linearly with frequency will produce no third-order or higher-order distortions, and that balanced detection will suppress the remaining second harmonics. For sufficient optical powers and balanced detection, the link is phase noise-limited and the NF is shown to be independent of the DC level. We also quantify the effect of the laser's residual IM on the distortion and find that it is significant.

To demonstrate a highly linear FM-DD link, we propose an FM discriminator design using tenth-order finite-impulse response (FIR) filters implemented in PLC. Figures-of-merit are calculated for this FM-DD link and compared to a link using an MZI discriminator. We demonstrate a 31 dB improvement in OIP3 over the MZI. To study the effect of filter fabrication variations on the linearity of the link, a Monte Carlo simulation is performed which varies coupling ratio errors and phase errors of the filter. The simulation shows that tolerances are tightly constrained. This offers both a challenge and an opportunity from progress in adaptive PLCs, which could bring about analog fiber optic links with very low distortion and large dynamic ranges.

II. ANALYSIS

A. Signal to Noise Ratio

A diagram of an FM-DD link is shown in Fig. 1. It consists of an FM laser, an optical filter and a photodetector. The source's residual IM and the filter's nonlinearities are the main contributors to distortion on the link. To quantify the nonlinearities, we

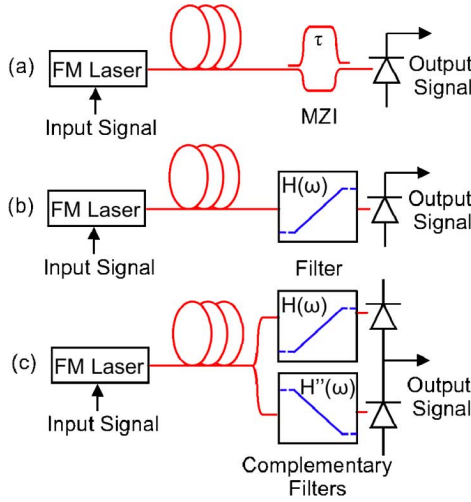


Fig. 1. FM-DD link consisting of a FM laser to convert microwave signals to optical frequency deviations, an FM discriminator to convert frequency deviations to intensity deviations, and a photodetector to convert IM back to electrical signals. In (a), the discriminator is an MZI. In (b), the discriminator is a linear filter. In (c), complementary linear filters and balanced detection are used to suppress second-order distortion.

apply a two-tone distortion test. An optical signal that is phase or frequency modulated by two sinusoidal tones can be represented by the time varying electric field

$$e(t) = \sqrt{2P_{\text{opt}}}\cos[\omega_c t + \beta_1 \sin(\omega_1 t) + \beta_2 \sin(\omega_2 t)] \quad (1)$$

where P_{opt} is the rms optical power, ω_c is the angular frequency of the optical carrier, β_1 and β_2 are the angle modulation depths, ω_1 and ω_2 are the modulation angular frequencies. For FM, each modulation depth is equal to the maximum optical frequency deviation of the carrier induced by the modulation divided by the frequency of the modulation, $\beta = \delta_\omega/\omega$. The instantaneous frequency of the light is

$$\omega_c + \delta_{\omega_1} \cos(\omega_1 t) + \delta_{\omega_2} \cos(\omega_2 t). \quad (2)$$

An FM laser is non-ideal as it produces undesired residual IM and includes noise. The correction to the electric field is

$$e(t) = a(t) + \sqrt{2P_{\text{opt}}(1 + n(t))} \cdot \sqrt{(1 + m_1 \cos(\omega_1 t + \phi) + m_2 \cos(\omega_2 t + \phi))} \cdot \cos[\omega_c t + \beta_1 \sin(\omega_1 t) + \beta_2 \sin(\omega_2 t) + \varphi(t)] \quad (3)$$

where $n(t)$ is the RIN of the source, $\varphi(t)$ is the phase noise of the source, $a(t)$ is the ASE noise from an optical amplifier, m represents the residual IM depth and φ is the phase difference between the IM and frequency modulation. The link will also amplify thermal noise present at the input.

An arbitrary optical filter is used on the link to convert FM to IM. Using the Jacobi-Anger expansion, the electric field after the filter can be expressed as an infinite weighted sum over sidebands. Similar to [18], we employ the shorthand notation to describe the electric field transmission at each sideband

$$h_{n,p} \equiv H(\omega = \omega_c + n\omega_1 + p\omega_2) \quad (4)$$

where n and p are integer indices and H is the complex transfer function of the filter, representing its phase and amplitude response, including any insertion losses or optical amplifier gain.

After the filter, the light is incident upon a photodetector. The output current from the photodetector is derived in Appendix A and approximated for small modulation depth. The standard definitions of the output intercept points rely on this approximation. At the output of the photodetector, the dc and the signal current at the modulation frequency ω_1 are

$$i_{\text{DC}} = RP_{\text{opt}}|X_0|^2, \quad (5)$$

$$i_{\omega_1} = RP_{\text{opt}}\text{Re}\left\{\left[\beta_1 X_1 + \frac{1}{2}m_1 Y_1 e^{j\phi}\right] \cdot \exp[j\omega_1 t]\right\} \quad (6)$$

where R is the responsivity of the photodetector, j is the imaginary unit, $\text{Re}\{\}$ means the real part, and for convenience we define the complex constants

$$X_0 = h_{0,0} \quad (7)$$

$$X_1 = h_{1,0}h_{0,0}^* - h_{0,0}h_{-1,0}^* \quad (8)$$

$$Y_1 = h_{1,0}h_{0,0}^* + h_{0,0}h_{-1,0}^* \quad (9)$$

$$X_2 = h_{2,0}h_{0,0}^* - 2h_{1,0}h_{-1,0}^* + h_{0,0}h_{-2,0}^* \quad (10)$$

$$X_3 = -h_{2,-1}h_{0,0}^* + h_{2,0}h_{0,1}^* + 2h_{1,-1}h_{-1,0}^* - 2h_{1,0}h_{-1,1}^* - h_{0,-1}h_{-2,0}^* + h_{0,0}h_{-2,1}^* \quad (11)$$

A passive link with no amplification will be considered, so the primary noises seen at the detector are shot, thermal, phase and RIN. The shot noise spectral density is proportional to the dc from the photodetector

$$S_{\text{SN}} = 2qI_{\text{DC}}R_{\text{load}} = 2qRP_{\text{opt}}|X_0|^2R_{\text{load}} \quad (12)$$

where q is the elementary charge and R_{load} is the load resistance at the output. The thermal noise spectral density is

$$S_{\text{TN}} = k_B T \quad (13)$$

where k_B is Boltzmann's constant and T is the temperature. The phase noise on the optical carrier is white noise with spectral density proportional to the laser's 3-dB linewidth, $\Delta\nu$. The phase fluctuations are converted to intensity fluctuations by the filter in the same manner as it converts the modulation. From [8], the average phase fluctuations in a small bandwidth near some frequency, f , are

$$\langle\varphi(t)^2\rangle \approx \frac{\Delta\nu}{\pi} \frac{\Delta f}{f^2} = \Delta\nu \frac{4\pi\Delta f}{\omega^2}. \quad (14)$$

Near the first modulation frequency, ω_1 , the output spectral density of the phase noise is

$$S_{\text{PN}} \approx R_{\text{load}}R_{\text{opt}}^2P_{\text{opt}}^24\pi\Delta\nu\omega_1^{-2}|X_1|^2. \quad (15)$$

The modulation is assumed to be below the relaxation frequency of the laser, so the RIN is modeled as white noise. The power spectral density of the noise at the output, near the modulation frequency is

$$S_{\text{IN}} \approx \frac{1}{4}R_{\text{load}}R_{\text{opt}}^2P_{\text{opt}}^2 \frac{\langle n(t)^2 \rangle}{B} |Y_1|^2 \quad (16)$$

where B is the bandwidth in Hz. The total noise power is

$$P_{\text{noise}} \approx (S_{SN} + S_{TN} + S_{PN} + S_{IN}) \cdot B. \quad (17)$$

The rms power into the load is

$$P_{\omega_1} = \frac{1}{2} R_{\text{load}} R^2 P_{\text{opt}}^2 \delta_{\omega_1}^2 \omega_1^{-2} |X_1|^2. \quad (18)$$

The SNR is $P_{\omega_1}/P_{\text{noise}}$. If the SNR is phase noise-limited, which is the case for sufficient optical powers, moderate RIN, and efficient conversion of phase fluctuations into intensity fluctuations, the SNR is given by

$$\text{SNR} = \delta_{\omega_1}^2 / 8\pi \Delta\nu B. \quad (19)$$

For FM discriminators that have constant conversion efficiency over a large enough bandwidth, the upper bound on the SNR for an FM-DD link is determined solely by the modulation depth and linewidth of the FM laser.

B. Distortion

The signal distortion caused by the FM-DD link can be described by the output power at frequencies that are harmonics and mixing terms of the modulation frequencies. For now, we assume there is no residual IM. The current component at frequency $2\omega_1 - \omega_2$ is

$$i_{2\omega_1 - \omega_2} = R P_{\text{opt}} \frac{1}{8} \beta_1^2 \beta_2 \text{Re}\{X_3 \exp[j(2\omega_1 - \omega_2)t]\}. \quad (20)$$

This third-order intermodulation product (IM3) outputs a power into the load of

$$P_{2\omega_1 - \omega_2} = \frac{1}{128} R_{\text{load}} R^2 P_{\text{opt}}^2 \delta_{\omega_1}^4 \omega_1^{-4} \delta_{\omega_2}^2 \omega_2^{-2} \cdot |X_3|^2. \quad (21)$$

If each of the two tones has an equal frequency modulation depth, $\delta_{\omega_1} = \delta_{\omega_2} = \delta_{\omega}$, the IMD's power is equal to the signal power for modulation depth

$$\delta_{\omega}^2 = 8\omega_1 \omega_2 |X_1| / |X_3|. \quad (22)$$

The corresponding OIP3 is

$$\text{OIP3} = 4R_{\text{load}} R^2 P_{\text{opt}}^2 \omega_1^{-1} \omega_2 |X_1|^3 / |X_3|. \quad (23)$$

The current component at frequency $2\omega_1$ is

$$i_{2\omega_1} = \frac{1}{4} R P_{\text{opt}} \beta_1^2 \text{Re}\{X_2 \exp[j2\omega_1 t]\}. \quad (24)$$

This second-order distortion outputs a power of

$$P_{2\omega_1} = \frac{1}{32} R_{\text{load}} R^2 P_{\text{opt}}^2 \delta_{\omega_1}^4 \omega_1^{-4} \cdot |X_2|^2. \quad (25)$$

This power is equal to the signal power for modulation depth

$$\delta_{\omega}^2 = 16\omega_1^2 |X_1|^2 / |X_2|^2. \quad (26)$$

The corresponding OIP2 is

$$\text{OIP2} = 8R_{\text{load}} R^2 P_{\text{opt}}^2 |X_1|^4 / |X_2|^2. \quad (27)$$

For an arbitrary filter, the distortion will depend on the particular modulation frequencies chosen. One desires to maximize X_1 and minimize X_2 and X_3 to reduce the distortion. A link with zero X_2 or X_3 will have infinite OIP2 or OIP3.

C. Spurious Free Dynamic Range

The SFDR is defined as the SNR at the maximum usable modulation depth. This can be defined when either the second-order or third-order distortion products breach the noise floor. For a phase noise-limited link, the IM3 is equal to the noise power at modulation depth

$$\delta_{\omega}^2 = (512\Delta\nu\pi\omega_1^2\omega_2^2B)^{1/3} |X_1|^{2/3} / |X_3|^{2/3}. \quad (28)$$

For a link limited by IM3, the SFDR is

$$\text{SFDR}_3 = \frac{(\omega_1\omega_2|X_1|)^{2/3}}{(\Delta\nu\pi B|X_3|)^{2/3}}. \quad (29)$$

For a phase noise-limited link, the power at the second-harmonic frequency is equal to the noise power at modulation depth

$$\delta_{\omega}^2 = 8\omega_1(2\Delta\nu\pi B)^{1/2} |X_1| / |X_2|. \quad (30)$$

For a link limited by the second-harmonic distortion, the SFDR is

$$\text{SFDR}_2 = \frac{2\omega_1|X_1|}{(2\Delta\nu\pi B)^{1/2}|X_2|}. \quad (31)$$

These figures-of-merit are often defined with respect to 1 Hz bandwidth. They generally depend on the particular modulation frequencies chosen. Maximizing the ratios of X_1/X_2 and X_1/X_3 will improve the dynamic range of the link.

III. FM DISCRIMINATOR DESIGN

Digital filter design techniques can be applied to the design of optical filters [22]. In general, one starts with a desired frequency response of the filter, which is written in terms of angular frequency $\Omega = -\pi$ to π , normalized over one free spectral range (FSR). Because the bandwidth of optical systems is very large, the optical spectrum can include many repeating periods of the response. One period of the filter is centered at a chosen center frequency ω_0 , which is not necessarily the same as the carrier frequency ω_c . We define the bias-frequency offset of the filter as $\omega_B = \omega_c - \omega_0$, which can be adjusted by tuning the wavelength of the transmitting laser or the physical parameters of the optical filter. The amplitude of the transfer function corresponds to the electric field transmission of the filter. The maximum bounds on the amplitude are -1 and 1 . Negative transmission corresponds to a phase shift at zero. The phase shifts between adjacent periods of the filter are determined by the filter type.

A. Mach-Zehnder Interferometer

The simplest filter used as an FM discriminator is an MZI with 50% coupling ratios. One arm of the interferometer has a

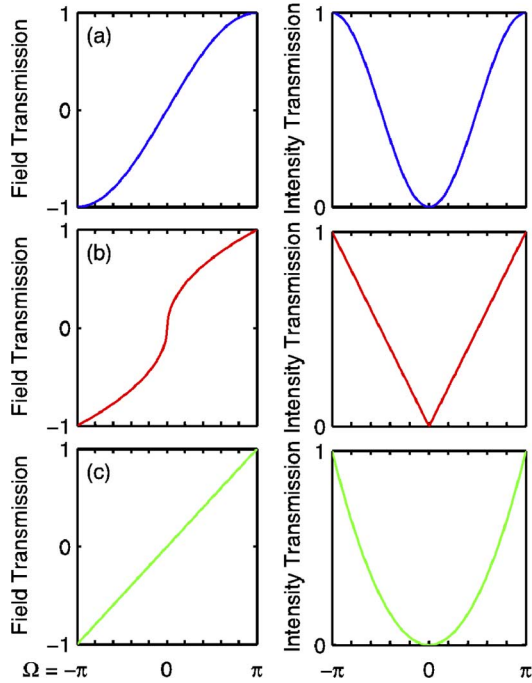


Fig. 2. Transfer functions for various optical filter designs. The filters are plotted over one FSR. The left column shows the amplitude or signed magnitude response for the electric field transmission. The right column shows the magnitude of the intensity transmission. Phase responses are not shown.

time shift with respect to the second arm. A normalized period of the filter is written as

$$h(\Omega) = \frac{1}{2} - \frac{j}{2} \exp[-j\Omega]. \quad (32)$$

This is plotted in Fig. 2(a). The filter is typically biased at quadrature, giving in our notation, (4), a transfer function of

$$h_{n,p} = \frac{1}{2} - \frac{j}{2} \exp[-j(n\omega_1 + p\omega_2)\tau] \quad (33)$$

where τ is the time delay between the two arms. The intensity response is a sinusoid

$$h_{n,p}h_{n,p}^* = \frac{1}{2} \{1 - \sin[(n\omega_1 + p\omega_2)\tau]\}. \quad (34)$$

Using the transfer function, we evaluate the link constants

$$X_0 = \frac{1}{4}(1 - j) \quad (35)$$

$$X_1 = \frac{1}{2}j(1 - e^{-j\omega_1\tau}) \quad (36)$$

$$X_2 = 0 \quad (37)$$

$$X_3 = -\frac{1}{2}j(1 - e^{j\omega_2\tau})(1 - e^{j\omega_1\tau})^2 e^{-j2\omega_1\tau} \quad (38)$$

As expected, we find that there is no second-harmonic so that OIP2 is infinite. From (36), and using the approximation $\omega_1\tau, \omega_2\tau \ll 1$, the power at the fundamental frequency is

$$P_{\omega_1} = \frac{1}{8} R_{\text{load}} R^2 P_{\text{opt}}^2 \delta_{\omega_1}^2 \tau^2 \quad (39)$$

and the power at frequency $2\omega_1 - \omega_2$ is

$$P_{2\omega_1 - \omega_2} = \frac{1}{512} R_{\text{load}} R^2 P_{\text{opt}}^2 \delta_{\omega_1}^4 \delta_{\omega_2}^2 \tau^6. \quad (40)$$

From (23), the OIP3 of the quadrature biased MZI is

$$\text{OIP3} = R_{\text{load}} R^2 P_{\text{opt}}^2. \quad (41)$$

From (29), the phase noise-limited SFDR is

$$\text{SFDR}_3 = (\Delta\nu\pi \cdot B\tau^2)^{-2/3}. \quad (42)$$

The equation for OIP3 for the MZI is consistent with [23]. This confirms the link model used for the analysis. It should be emphasized that both the useful bandwidth and the SFDR are improved by having a short time delay.

B. Linear Intensity

A number of groups have proposed or built optical filters that have a transfer function linear in optical intensity versus frequency and small group delay [13]–[20]. Within one-half period, the transfer function can be represented by

$$h_{n,p} = \sqrt{A \cdot (\omega_B + n\omega_1 + p\omega_2)} e^{-j\tau(\omega_B + n\omega_1 + p\omega_2)} \quad (43)$$

where A is a slope in units of inverse angular frequency and τ is a time delay. The intensity response is

$$h_{n,p}h_{n,p}^* = A \cdot (\omega_B + n\omega_1 + p\omega_2) \quad (44)$$

which is linear in slope A . The field and intensity responses are illustrated in Fig. 2(b). Using the transfer function, we evaluate the link constants

$$X_0 = \sqrt{A \cdot \omega_B} e^{-j\tau\omega_B} \quad (45)$$

$$X_1 = A\omega_B [\sqrt{1 + (\omega_1/\omega_B)} - \sqrt{1 - (\omega_1/\omega_B)}] e^{-j\tau\omega_1} \quad (46)$$

$$X_2 = A\omega_B [\sqrt{1 + 2(\omega_1/\omega_B)} + \sqrt{1 - 2(\omega_1/\omega_B)} - 2\sqrt{1 + (\omega_1/\omega_B)}\sqrt{1 - (\omega_1/\omega_B)}] e^{-j2\tau\omega_1} \quad (47)$$

$$X_3 = A\omega_B [2\sqrt{1 + (\omega_1/\omega_B)} - (\omega_2/\omega_B) \times \sqrt{1 - (\omega_1/\omega_B)} - 2\sqrt{1 - (\omega_1/\omega_B)} + (\omega_2/\omega_B)\sqrt{1 + (\omega_1/\omega_B)}] \times \sqrt{1 - 2(\omega_1/\omega_B)} + (\omega_2/\omega_B) - \sqrt{1 + 2(\omega_1/\omega_B)} - (\omega_2/\omega_B) + \sqrt{1 + 2(\omega_1/\omega_B)}\sqrt{1 + (\omega_2/\omega_B)} - \sqrt{1 - 2(\omega_1/\omega_B)}\sqrt{1 - (\omega_2/\omega_B)}] e^{-j\tau(2\omega_1 - \omega_2)}. \quad (48)$$

Generally, X_2 and X_3 are non-zero for this discriminator, even if the square roots are expanded. This means that an FM discriminator that is linear in optical intensity will still produce second-order and third-order distortion. Coherent mixing in the photodetector produces cross terms that are not eliminated. A coherent FM discriminator that is linear in optical intensity will not produce a distortion-less link.

C. Linear Electric Field

The ideal filter for an FM-DD link is an optical filter that is linear in electric field. We find that this filter has second order-distortion that is produced by the square-law detection, but no other higher-order distortion. Within one period, the field transmission ramps linearly with frequency, and the filter has linear phase. The filter's field and intensity transfer functions are shown in Fig. 2(c). The transfer function is

$$h_{n,p} = A \cdot (\omega_B + n\omega_1 + p\omega_2) e^{-j\tau(\omega_B + n\omega_1 + p\omega_2)} \quad (49)$$

where A is a slope and τ is a time delay. In the intensity domain, the filter looks quadratic

$$h_{n,p} h_{n,p}^* = A^2 \cdot (\omega_B + n\omega_1 + p\omega_2)^2. \quad (50)$$

The link constants are

$$X_0 = A\omega_B \exp[-j\tau\omega_B] \quad (51)$$

$$X_1 = 2\omega_1 \cdot A^2\omega_B \exp[-j\tau\omega_1] \quad (52)$$

$$X_2 = \omega_1^2 A^2 \exp[-j\tau 2\omega_1] \quad (53)$$

$$X_3 = 0. \quad (54)$$

Using (5) and (50), we find the dc at the output of the photodetector

$$i_{DC} = RP_{\text{opt}}(A^2\omega_B^2) \equiv RP_{\text{opt}}D^2 \quad (55)$$

where we define the constant D to describe the dc bias. D^2 is the fraction of optical power transmitted by the filter at the optical carrier frequency. From (6) and (51), the current component at the fundamental frequency ω_1 is

$$i_{\omega_1} = 2RDP_{\text{opt}}A\delta_{\omega_1} \cos[\omega_1(t - \tau)]. \quad (56)$$

The magnitude of the output current is linearly proportional to the slope of the filter and linearly proportional to the frequency modulation depth δ_{ω} . This filtered link produces distortion at the second-harmonic of each modulation tone. The distortion is caused by the first-order sidebands beating with each other. The current component at frequency $2\omega_1$ is

$$i_{2\omega_1} = \frac{1}{2}RP_{\text{opt}}A^2\delta_{\omega_1}^2 \cos[2\omega_1(t - \tau)]. \quad (57)$$

The second-harmonic can be suppressed if the output of the optical system is detected using balanced detection, as shown in Fig. 1(c). The filter before the second photodetector is designed to have a slope complementary to the filter in (49). Its transfer function is

$$h''_{n,p} = A(\omega_B - n\omega_1 - p\omega_2) e^{-j\tau(\omega_B + n\omega_1 + p\omega_2)}. \quad (58)$$

The current component at the fundamental frequency will be 180° out of phase between the two photodetectors, but the second-harmonic will be in phase. Subtracting the second current from the first, the second-harmonic will cancel.

In the small modulation depth approximation, this ideal FM-DD link has no other higher-order distortion. At a given harmonic, sum or difference frequency, if all the sidebands in the sum in (A6) corresponding to that frequency fall within a region of the filter that closely approximates the desired

linear ramp function, the output current is zero. The ideal link will have infinite OIP2 and in-band OIP3 if both the negative and positive second-order sidebands fall within this region. Using a symbolic algebra solver, we verified that the current is zero for all intermodulation frequencies up to sixth-order. Additional sources of nonlinearity are the frequency modulated laser source, optical fibers and photodetector. For sufficient modulation depth, the dominant FM sidebands will fall outside the bandwidth of the filter and this saturation will cause nonlinearities.

IV. OPTIMIZATION OF THE LINEAR LINK

A. Gain, Noise Figure and Low Biasing

Low biasing the filter, meaning that ω_c is very close to the zero transmission point at ω_0 , is suggested to improve the NF of the link [16]. There is a tradeoff between decreasing the dc, which decreases shot noise, and reducing the signal gain, so an optimal bias point must be found. The filter cannot be biased exactly at the null or the link would have zero output current, since we find in (56) that the output is proportional to the bias. This is consistent with our experience with carrier suppression on IM-DD links.

Using (12), the noise contribution from shot noise is

$$S_{SN} = 2qRP_{\text{opt}}D^2R_{\text{load}}. \quad (59)$$

The noise contribution from optical phase noise is

$$S_{PN} = 8\pi R_{\text{load}}R^2P_{\text{opt}}^2\Delta\nu A^2D^2. \quad (60)$$

The rms output power of the link, from squaring the current in (56) is

$$P_{\omega_1} = 2R_{\text{load}}R^2D^2P_{\text{opt}}^2A^2\delta_{\omega_1}^2. \quad (61)$$

The frequency modulation depth in terms of the FM laser parameters can be written as

$$\delta_{\omega_1}^2 = (2\pi\eta \cdot i_{\text{in}})^2 = 2(2\pi\eta)^2 P_{\text{in}}/R_{\text{load}} \quad (62)$$

where η is the FM laser's modulation efficiency in Hz/A, typically of the order of a few hundred MHz per mA, i_{in} is the peak input current, and P_{in} is the rms input power. Assuming equal input and output loads, the power gain of the link is

$$G = 16R^2D^2P_{\text{opt}}^2A^2\pi^2\eta^2. \quad (63)$$

To minimize the NF for a given optical power, one wishes to maximize the ratio of the gain to the noise. Including thermal noise at the input and output, the NF can be written as

$$\text{NF} = 1 + \frac{1}{G} + R_{\text{load}} \frac{q + 4\pi RP_{\text{opt}}\Delta\nu A^2}{8RP_{\text{opt}}A^2\pi^2\eta^2 k_B T}. \quad (64)$$

From inspection, we see that the noise figure is not improved by low biasing the filter, and a high bias is desirable to maintain the gain. For high optical powers, the limit on the NF is

$$\text{NF} = 1 + \Delta\nu R_{\text{load}} / (2\pi k_B T \eta^2). \quad (65)$$

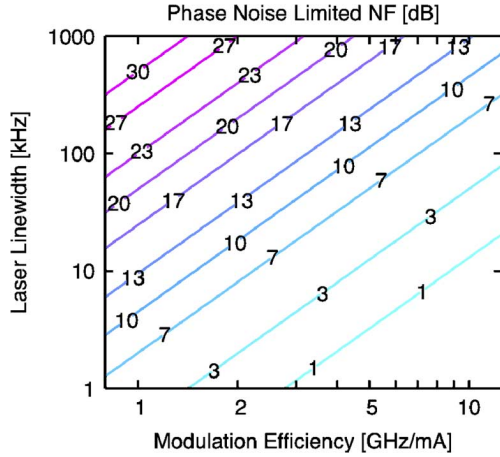


Fig. 3. Phase noise limited noise figure for an FM-DD link with high optical power as a function of laser linewidth and modulation efficiency.

This is independent of the filter bias and the slope of the filter. The dominant noise term is the laser phase noise. Fig. 3 shows the phase noise-limited NF as a function of linewidth and modulation efficiency.

B. Residual Intensity Modulation

Residual IM sets a lower limit on the distortion for an ideal balanced-detection FM-DD link. Taking residual IM into account, from (A10), the current component at the IM3 frequency $2\omega_1 - \omega_2$ is

$$i_{2\omega_1 - \omega_2}^b = \frac{1}{8} R P_{\text{opt}} \left(A^2 \delta_{\omega_1} m_1 \delta_{\omega_2} + \frac{1}{4} D A m_1^2 \delta_{\omega_2} \right) \times \cos[(2\omega_1 - \omega_2)(t - \tau)] \quad (66)$$

where the superscript b indicates that the current is at the output of the balanced detectors. We can normalize the IM depth to the FM depth

$$M \equiv m / \delta_{\omega}. \quad (67)$$

If each tone has an equal frequency modulation depth, the IMD's power is equal to the signal for modulation depth

$$\delta_{\omega}^2 = 16D / \left(A M + \frac{1}{4} D M^2 \right). \quad (68)$$

The corresponding OIP3 is

$$\text{OIP3} = 32 R_{\text{load}} R_{\text{opt}}^2 P_{\text{opt}}^2 D^3 A^2 / \left(A M + \frac{1}{4} D M^2 \right). \quad (69)$$

From (A9), the current component at the second-harmonic frequency $2\omega_1$ is

$$i_{2\omega_1}^b = R D P_{\text{opt}} A m_1 \delta_{\omega_1} \cos[2\omega_1(t - \tau)]. \quad (70)$$

The second-harmonic is equal to the signal power for modulation depth

$$\delta_{\omega}^2 = 4 / M^2. \quad (71)$$

The corresponding OIP2 is

$$\text{OIP2} = 8 R_{\text{load}} R_{\text{opt}}^2 P_{\text{opt}}^2 A^2 D^4 / M^2. \quad (72)$$

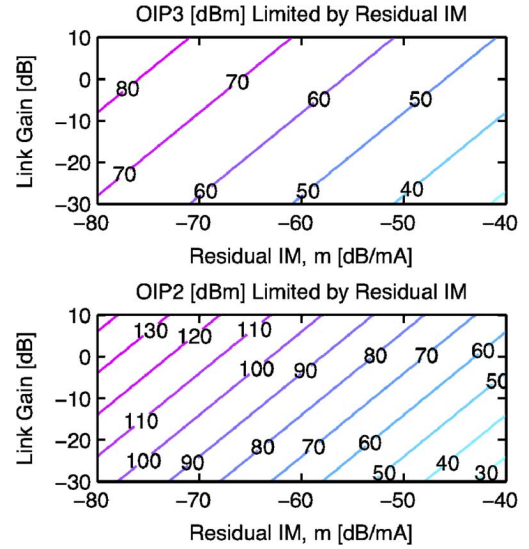


Fig. 4. OIP3 and OIP2 versus gain and residual IM for 100 mW optical power, 2 GHz/mA nominal modulation efficiency, 50 ohm output impedance, 0.5 bias, 4 GHz maximum modulation frequency and detector responsivity of 0.8 A/W. The link's figures of merit can be improved by increasing the modulation efficiency, optical power, or responsivity.

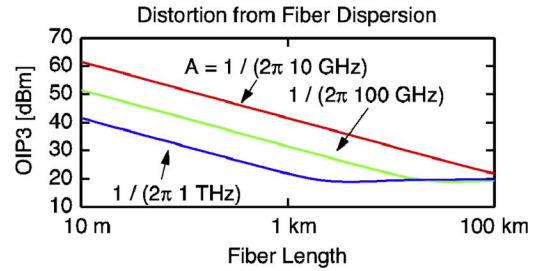


Fig. 5. OIP3 for ideal discriminator for different slope values, assuming standard SMF, $\beta_2 = -20$ ps²/km, 100 mW incident optical power, 50 ohm output impedance, detector responsivity of 0.8 A/W, 0.5 bias, and modulation frequencies of 2 GHz and 2.1 GHz.

Fig. 4 shows OIP3 and OIP2 as functions of link gain and residual IM, assuming a maximum modulation frequency of 4 GHz, bias of 0.5 and modulation efficiency of nominally 2 GHz/mA. For FM-DD links to exhibit superior third-order and second-order distortion performance, the FM laser must be optimized for low residual IM.

C. Fiber Dispersion

The dispersion of the optical fiber also increases the distortion of an FM-DD link. The dispersion is modeled by multiplying the filter transfer function by the term $\exp[-j\beta_2 z(n\omega_1 + p\omega_2)^2/2]$, where β_2 is the fiber dispersion parameter and z is the fiber length. Fig. 5 shows that the dispersion sets an upper limit on OIP3, degrading by 10 dB per decade of fiber length. This can be corrected by using a length of dispersion compensated fiber, or by designing a discriminator filter's transfer function to include the inverse of the dispersion.

V. PLC IMPLEMENTATION

A FM discriminator approximating the ideal linear field response can be constructed using PLC. The transform function

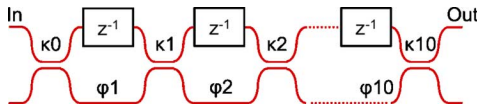


Fig. 6. FIR lattice filter architecture, indicating for each stage the coupling coefficients, designated by κ , and phase shifts, designated by φ . Each stage has a unit delay, z^{-1} . The dashed lines indicate additional filter stages omitted from the figure.

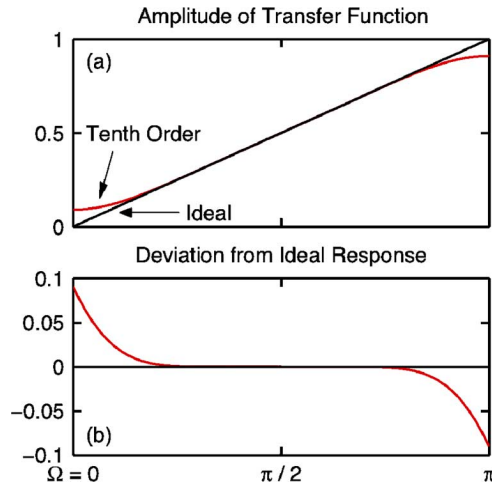


Fig. 7. (a) Amplitude response of the tenth-order maximally flat FIR filter over one FSR compared to the ideal response. (b) Deviation from the ideal response.

of an arbitrary digital filter with all zeros in its z -transform representation, called a FIR or moving average (MA) filter, can be realized in PLC with just MZIs and directional couplers. FIR filters work well as FM discriminators because they can be designed to have exactly linear phase.

One implementation of a multi-stage optical FIR filter in PLC is the lattice filter. The lattice filter architecture has a low-loss passband and requires only $N + 1$ couplers for an N stage filter, which are advantages over other optical filter architectures [25]. The lattice architecture is shown in Fig. 6. A recursion relation exists that transforms between given digital filter coefficients and the corresponding coupling ratios and phase shifts [22].

A physically-realized filter is limited in its number of stages. Therefore, it will only closely approximate the desired linear frequency response. We find that good performance can be obtained from filters designed using the maximally linear criteria developed for digital differentiators by [26]–[28]. The maximally linear criteria fixes the amplitude, slope and a number of higher derivatives of the filter transfer function at a chosen frequency. In our design, we choose filter coefficients that satisfy the maximally linear criteria at $\Omega = \pi/2$, and we bias the filter at that optimized frequency.

The coefficients of a tenth-order, maximally linear at $\Omega = \pi/2$, FIR filter are in Table I [27]. The transfer function and its deviation from an ideal linear ramp are shown in Fig. 7. The recursion relation for the lattice filter design gives 1024 solutions for a 10-stage filter. One particular solution is in Table II.

The third-order distortion for a link using the FIR filter is calculated using (23), and the second-order distortion using (27), which take into account the nonidealities in the transfer function. Assuming 100 mW of optical power, 50 ohm load resis-

TABLE I
FILTER COEFFICIENTS

Coefficient	Value	Coefficient	Value
a0	-0.000746	a6	-0.1865
a1	0	a7	0
a2	-0.01036	a8	-0.01036
a3	0	a9	0
a4	-0.1865	a10	-0.000746
a5	0.5		

Coefficients for the tenth-order FIR filter in Z transform representation.

TABLE II
FILTER DESIGN PARAMETERS

Coupling Ratio	Value	Phase Shift	Value
κ_0	0.6743	φ_1	0
κ_1	0.6355	φ_2	$-\pi$
κ_2	0.8375	φ_3	0
κ_3	0.5148	φ_4	$-\pi$
κ_4	0.9185	φ_5	0
κ_5	0.5386	φ_6	0
κ_6	0.9184	φ_7	$-\pi$
κ_7	0.5152	φ_8	0
κ_8	0.8373	φ_9	$-\pi$
κ_9	0.6358	φ_{10}	$-\pi$
κ_{10}	0.3257		

Coupling ratios and phase shifts for each stage of the tenth-order FIR lattice filter.

tance and 0.8 A/W responsivity, we sweep over the possible modulation frequencies. Plots of OIP3 and OIP2 versus modulation maximum frequency are shown in Fig. 8. If the modulation frequency is limited to 0.5% of the FSR, then the tenth-order filter has a worst case OIP3 of 56 dBm, which is 31 dB better than a MZI. For 4 GHz RF bandwidth, one would choose a 800 GHz FSR for the filter, corresponding to a 1.25 ps unit delay for each stage, or a differential length of approximately 258 μm , assuming $n = 1.45$ for silica. It is important to note the gain-bandwidth tradeoff, as increasing the FSR will increase the bandwidth but decrease the slope of the filter and thus the gain of the link. If a specified gain is desired, there is a tradeoff between distortion and bandwidth.

We perform a Monte-Carlo simulation to study the effect of fabrication variations on the resulting distortions of the filter. When each coupling coefficient and phase shift is varied, the new filter coefficients are calculated, and the resulting OIP3 and OIP2 are calculated. In our first simulation, a set of maximum relative coupling coefficient errors were chosen, and 100 trials were performed for each. In each trial, the random variation for each coupling was uniformly distributed from minus to plus the maximum error. Fig. 9 shows that OIP3 and OIP2 degrade significantly if the coupling ratios are not controlled to within 0.1% of the designed values. In a second simulation, a set of maximum phase errors were chosen, and 100 trials were performed for each. Fig. 10 shows that OIP3 degrades significantly if phases are not controlled to within 0.01 radians of their designed values. OIP2 is much more sensitive to phase errors than OIP3 because the phase difference between the two photodetectors determines the cancellation of the second harmonics.

PLC filter technology is slowly maturing. Silica waveguides on silicon substrates have been fabricated with low loss and

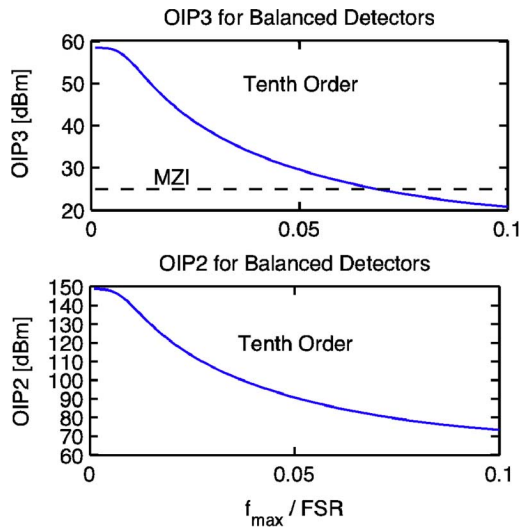


Fig. 8. OIP3 and OIP2 for the tenth-order FIR filter versus maximum modulation frequency normalized to the FSR of the filter. There is 100 mW optical power, 50 ohm output impedance, and responsivity of 0.8 A/W. Limiting the modulation frequency increases the performance. OIP3 for a MZI filter is shown on the same plot.

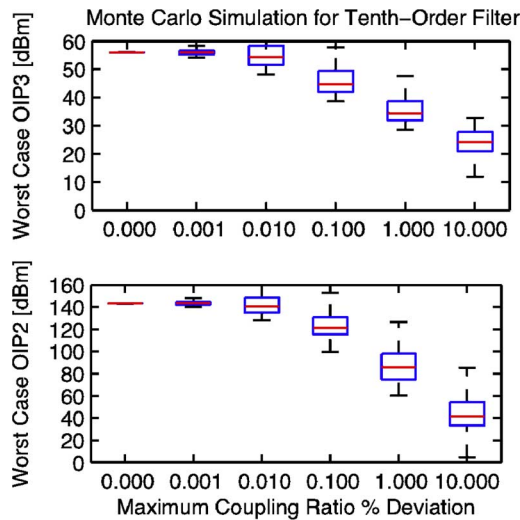


Fig. 9. Monte Carlo simulation of the effect of coupling ratio errors on the resulting OIP3 and OIP2 of the balanced link using the tenth-order FIR filter. The box plots indicate the mean, 25th and 75th percentiles for each simulation consisting of 100 trials. The whiskers represent the maximum and minimum values.

good repeatability, and commercial quality high-order IIR filters have been demonstrated past tenth-order [24]. The tight tolerances for this particular lattice filter implementation pose challenges for fabrication and temperature stability, however practical high order optical FIR filters have been successfully demonstrated using feedback control. A thermally tuned, sixth-order FIR filter with 100 GHz FSR used for adaptive equalization has been reported in literature [30].

To use this thermal tuning technique, we are exploring algorithms to tune the phases of each stage with different feedback signals from the electrical domain. The waveguide coupling, which depends exponentially on the separation between

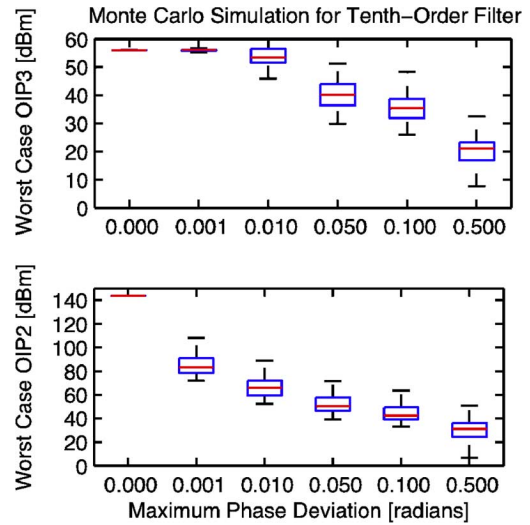


Fig. 10. Monte Carlo simulation of the effect of phase errors.

the waveguides, cannot be easily tuned. Vertical coupling between waveguides, which has found applications with microresonators [29], may offer the best control over coupling accuracy, since layer thicknesses in fabrication can be controlled to nanometer scale. The coupling ratios should be controllable to less than 0.1%. In addition, we are exploring other architectures or filter designs which may be more robust.

VI. CONCLUSION

We have derived figures of merit for FM-DD analog fiber optic links with arbitrary FM discriminator filters. The theory is shown to be consistent with previous work on MZIs. To the best of our knowledge, we are the first to propose balanced FM discriminator filters that are linear in field transmission versus frequency to obtain highly linear FM-DD links. Theory on the effect of residual IM is developed, and it shown that constraining intensity deviations to less than 0.005% for 1 GHz of frequency deviation will ensure great distortion performance. Low biasing the filter is shown to not improve the NF of the link.

We have presented one physical implementation of a linear FM discriminator using a tenth-order FIR lattice filter fabricated with PLC. Filter coefficients chosen using the maximally linear criteria have good distortion performance. The filter outperforms the MZI in third order distortion by 31 dB, and obtains an OIP3 of 56 dBm for 100 mW of optical power, 0.8 A/W photodetector responsivity and a 4 GHz bandwidth. Fabrication constraints on the linear filter have been analyzed using Monte-Carlo simulations. The phases on each stage of the filter must be constrained to about 0.01 radians from the designed values, and the coupling ratios to 0.1% of their designed values.

The proposed FM-DD analog fiber optic link offers an opportunity for continued optimization. The implementation of high order maximally linear filters will become a reality with continuing progress in PLC fabrication and tuning techniques, which will allow FM-DD links to surpass IM links in linearity. FM-DD links are a promising choice for low distortion, high dynamic range transmission of analog signals.

APPENDIX A
DERIVATION OF OUTPUT CURRENTS

The electric field at the output of the modulated laser diode is given by (3). The residual IM depth, m , and the intensity noise, $n(t)$, are small so the square root can be expanded using a Taylor series, yielding

$$e(t) \approx a(t) + \sqrt{2P_{\text{opt}}} \cdot \left(1 + \frac{1}{2}m_1 \cos(\omega_1 t + \phi) + \frac{1}{2}m_2 \cos(\omega_2 t + \phi) + \frac{1}{2}n(t) \right) \cdot \cos[\omega_c t + \beta_1 \sin(\omega_1 t) + \beta_2 \sin(\omega_2 t) + \varphi(t)]. \quad (\text{A1})$$

The signal passes through the FM discriminator filter. Ignoring noise, the electric field after the filter is

$$e(t) = \sqrt{2P_{\text{opt}}} \text{Re} \left\{ \sum_{n=-\infty}^{\infty} \sum_{p=-\infty}^{\infty} j_{n,p} e^{j(\omega_c + n\omega_1 + p\omega_2)t} \right\}, \quad (\text{A2})$$

where we define

$$j_{n,p} \equiv h_{n,p} J_n(\beta_1) J_p(\beta_2) + \frac{1}{4} h_{n,p} m_1 [J_{n-1}(\beta_1) e^{j\phi} + J_{n+1}(\beta_1) e^{-j\phi}] J_p(\beta_2) + \frac{1}{4} h_{n,p} m_2 J_n(\beta_1) [J_{p-1}(\beta_2) e^{j\phi} + J_{p+1}(\beta_2) e^{-j\phi}] \quad (\text{A3})$$

where J is a Bessel function of the first kind and j without a subscript is the imaginary unit.

The electric field in (A2) is incident upon a photodetector at the termination of a fiber-optic link. The photodetector is assumed to be an ideal square-law detector operating in its linear region with responsivity R . The output current is

$$i(t) = RP_{\text{opt}} \text{Re} \left\{ \sum_{n=-\infty}^{\infty} \sum_{p=-\infty}^{\infty} \sum_{g=-\infty}^{\infty} \sum_{k=-\infty}^{\infty} j_{n,p} j_{g,k}^* \times \exp[j((n-g)\omega_1 + [p-k]\omega_2)t] \right\}. \quad (\text{A4})$$

Combining like terms, this rearranges to

$$i(t) = RP_{\text{opt}} \sum_{g=-\infty}^{\infty} \sum_{k=-\infty}^{\infty} \text{Re} \left\{ |j_{g,k}|^2 + 2 \sum_{n=1}^{\infty} j_{n+g,k} j_{g,k}^* \exp[jn\omega_1 t] + 2 \sum_{p=1}^{\infty} j_{g,p+k} j_{g,k}^* \exp[jp\omega_2 t] + 2 \sum_{n=1}^{\infty} \sum_{p=1}^{\infty} j_{n+g,p+k} j_{g,k}^* \exp[j(n\omega_1 + p\omega_2)t] + 2 \sum_{n=1}^{\infty} \sum_{p=1}^{\infty} j_{n+g,-p+k} j_{g,k}^* \exp[j(n\omega_1 - p\omega_2)t] \right\} \quad (\text{A5})$$

where the asterisk denotes the complex conjugate and $\text{Re}\{\}$ means the real part. The double-sum over indices g and k gives the contribution of each pair of optical sidebands that beat together to produce the output current. In this form, the current is separated into different frequency components, which are indicated by the summation indices n and p . The first term, where n and p are both identically zero, gives the dc. The second term, a summation over the index n , gives the fundamental tone at angular frequency ω_1 and its harmonics. The third term, a summation over the index p , gives the fundamental tone at angular frequency ω_2 and its harmonics. The fourth term is the sum frequencies produced by the mixing, and the fifth term is the difference frequencies produced by the mixing.

For small modulation depth, $\beta \ll 1$, and no residual IM, $m = 0$, the Bessel functions can be approximated by $J_0(z) \approx 1$ and $J_n(z) \approx (z/2)^{|n|}/|n|!$, for positive n , noting that $J_{-n}(z) = (-1)^n J_n(z)$. Keeping terms of lowest polynomial order, the current simplifies to the following equation:

$$i(t) \approx RP_{\text{opt}} \text{Re} \left\{ |h_{0,0}|^2 + 2 \sum_{n=1}^{\infty} \sum_{g=0}^n \frac{\beta_1^n}{2^n} \frac{(-1)^g}{(n-g)!g!} h_{n-g,0} h_{-g,0}^* \exp[jn\omega_1 t] + 2 \sum_{p=1}^{\infty} \sum_{k=0}^p \frac{\beta_2^p}{2^p} \frac{(-1)^k}{(p-k)!k!} h_{0,p-k} h_{0,-k}^* \exp[jp\omega_2 t] + 2 \sum_{n=1}^{\infty} \sum_{p=1}^{\infty} \sum_{g=0}^n \sum_{k=0}^p \frac{\beta_1^n \beta_2^p}{2^{n+p}} \frac{(-1)^{p+g+k}}{(n-g)!g!(p-k)!k!} \cdot h_{n-g,-p+k} h_{-g,k}^* \exp[j(n\omega_1 - p\omega_2)t] \right\}. \quad (\text{A6})$$

There are four current components of interest. The amplitude of the dc, as should be expected, is proportional to the optical power in the optical carrier after the filter

$$i_{\text{DC}} = RP_{\text{opt}} |h_{0,0}|^2. \quad (\text{A7})$$

The current at the fundamental frequency ω_1 is linearly proportional to the modulation depth. It depends on the negative and positive first-order sidebands beating with the optical carrier. The current component is

$$i_{\omega_1} = RP_{\text{opt}} \beta_1 \text{Re} \{ (h_{1,0} h_{0,0}^* - h_{0,0} h_{-1,0}^*) \exp[j\omega_1 t] \}. \quad (\text{A8})$$

The current at the second-harmonic frequency $2\omega_1$ has a quadratic relationship to modulation depth. It depends on the second-order sidebands beating with the optical carrier, as well as the first-order sidebands beating with each other. It is

$$i_{2\omega_1} = RP_{\text{opt}} \frac{1}{4} \beta_1^2 \text{Re} \{ (h_{2,0} h_{0,0}^* - 2h_{1,0} h_{-1,0}^* + h_{0,0} h_{-2,0}^*) \exp[j2\omega_1 t] \}. \quad (\text{A9})$$

The current produced at the difference frequency $2\omega_1 - \omega_2$ is a third-order intermodulation product. It is

$$i_{2\omega_1 - \omega_2} = RP_{\text{opt}} \frac{1}{8} \beta_1^2 \beta_2 \text{Re} \{ (-h_{2,-1} h_{0,0}^* + h_{2,0} h_{0,1}^* + 2h_{1,-1} h_{-1,0}^* - 2h_{1,0} h_{-1,1}^* - h_{0,-1} h_{-2,0}^* + h_{0,0} h_{-2,1}^*) \exp[j(2\omega_1 - \omega_2)t] \}. \quad (\text{A10})$$

The effect of residual IM can also be obtained from (A5). It is difficult to write a general expression, but it is possible to

expand some individual terms. In lowest polynomial order of the modulation depth, the same currents of interest are

$$i_{DC} \approx RP_{\text{opt}} |h_{0,0}|^2 \quad (\text{A11})$$

$$i_{\omega_1} \approx RP_{\text{opt}} \text{Re} \left\{ \left[\beta_1 (h_{1,0} h_{0,0}^* - h_{0,0} h_{-1,0}^*) + \frac{1}{2} m_1 (h_{1,0} h_{0,0}^* + h_{0,0} h_{-1,0}^*) e^{j\phi} \right] \cdot \exp[j\omega_1 t] \right\} \quad (\text{A12})$$

$$i_{2\omega_1} \approx RP_{\text{opt}} \frac{1}{4} \text{Re} \left\{ \left[\beta_1^2 (h_{2,0} h_{0,0}^* - 2h_{1,0} h_{-1,0}^* + h_{0,0} h_{-2,0}^*) + m_1 \beta_1 (h_{2,0} h_{0,0}^* - h_{0,0} h_{-2,0}^*) e^{j\phi} + \frac{1}{2} m_1^2 h_{1,0} h_{-1,0}^* e^{j2\phi} \right] \exp[j2\omega_1 t] \right\} \quad (\text{A13})$$

and

$$i_{2\omega_1 - \omega_2} \approx RP_{\text{opt}} \frac{1}{8} \text{Re} \left\{ \left[\beta_1^2 \beta_2 (-h_{2,-1} h_{0,0}^* + 2h_{1,-1} h_{-1,0}^* - h_{0,-1} h_{-2,0}^* + h_{2,0} h_{0,1}^* - 2h_{1,0} h_{-1,1}^* + h_{0,0} h_{-2,1}^*) + m_1 \beta_1 \beta_2 e^{j\phi} \times (h_{2,0} h_{0,1}^* + h_{2,-1} h_{0,0}^* + h_{0,-1} h_{-2,0}^* - h_{0,0} h_{-2,1}^*) + \frac{1}{2} m_2 \beta_1^2 e^{-j\phi} (h_{2,0} h_{0,1}^* + h_{2,-1} h_{0,0}^* - 2h_{1,0} h_{-1,1}^* - 2h_{1,-1} h_{-1,0}^* + h_{0,0} h_{-2,1}^* + h_{0,-1} h_{-2,0}^*) + \frac{1}{2} m_1^2 \beta_2 e^{j2\phi} (-h_{1,-1} h_{-1,0}^* + h_{1,0} h_{-1,1}^*) + \frac{1}{2} m_1 m_2 \beta_1 (h_{2,0} h_{0,1}^* + h_{1,-1} h_{-1,0}^* - h_{1,0} h_{-1,1}^* - h_{0,-1} h_{-2,0}^*) \right] \right\} \quad (\text{A14})$$

In a balanced-link architecture, the filter transfer function may be different for each arm. Half the optical power passes through each filter, so the current is decreased by one half.

REFERENCES

- [1] S. Pappert, C. Sun, R. Orazi, and T. Weiner, "Microwave fiber optic links for shipboard antenna applications," in *Proc. 2000 IEEE Int. Conf. Phased Array Syst. Technol.*, Dana Point, CA, pp. 345–348.
- [2] P. P. Smyth, "Optical radio—A review of a radical new technology for wireless access infrastructure," *BT Technol. J.*, vol. 21, no. 3, pp. 22–31, Jul. 2003.
- [3] J. Capmany and D. Novak, "Microwave photonics combines two worlds," *Nat. Photon.*, vol. 1, no. 6, pp. 319–330, June 2007.
- [4] C. Cox, E. Ackerman, R. Helkey, and G. Betts, "Direct-detection analog optical links," *IEEE Trans. Microw. Theory Tech.*, vol. 45, no. 8, pp. 1375–1383, Aug. 1997.
- [5] S. Matsuo, T. Kakitsuka, T. Segawa, N. Fujiwara, Y. Shibata, H. Oohashi, H. Yasaka, and H. Suzuki, "Extended transmission reach using optical filtering of frequency-modulated widely tunable SSG-DBR laser," *IEEE Photon. Technol. Lett.*, vol. 20, no. 2, pp. 294–296, Feb. 2008.
- [6] O. Ishida, H. Toba, and Y. Tohmori, "Pure frequency modulation of a multielectrode distributed-Bragg-reflector (DBR) laser diode," *IEEE Photon. Technol. Lett.*, vol. 1, no. 7, pp. 156–158, Jul. 1989.
- [7] Q. S. Xiang, Y. Zhao, and F.-S. Choa, "A high-performance RF-light-wave transmitter for analog fiber links," in *Proc. LEOS 2000, 13th Annu. Meeting*, vol. 1, pp. 138–139.

- [8] R. Kalman, J. Fan, and L. Kazovsky, "Dynamic range of coherent analog fiber-optic links," *J. Lightw. Technol.*, vol. 12, no. 7, pp. 1263–1277, Jul. 1994.
- [9] J. M. Roth, "Frequency modulated analog fiber optic links using direct detection," Master's thesis, MIT, Cambridge, May 1997.
- [10] S. E. Harris, "Conversion of FM light to AM light using birefringent crystals," *Appl. Phys. Lett.*, vol. 2, no. 3, pp. 47–49, 1963.
- [11] I. P. Kaminow, "Balanced optical discriminator," *Appl. Opt.*, vol. 3, no. 4, pp. 507–510, Apr. 1964.
- [12] W. Sorin, K. Chang, G. Conrad, and P. Hernday, "Frequency domain analysis of an optical FM discriminator," *J. Lightw. Technol.*, vol. 10, no. 6, pp. 787–793, Jun. 1992.
- [13] J. Chen and R. Brown, "Novel optical frequency discriminator with 'perfect' linearity," in *Proc. OFC, 2000*, vol. 2, pp. 329–331.
- [14] X. Xie, J. Khurgin, J. Kang, and F. Choa, "Compact linearized optical FM discriminator," *IEEE Photon. Technol. Lett.*, vol. 14, no. 3, pp. 384–386, Mar. 2002.
- [15] T. Darcie, J. Zhang, P. Driessen, and J. Eun, "Demonstration of a class-B microwave-photonic link using optical frequency modulation and complementary fiber-Bragg-grating discriminators," presented at the OFC/NFOEC, Anaheim, CA, 2006, Postdeadline Paper PDP38..
- [16] J. Zhang and T. Darcie, "Low-biased microwave-photonic link using optical frequency or phase modulation and fiber-Bragg-grating discriminator," presented at the OFC/NFOEC, Anaheim, CA, 2006, Paper OWG1.
- [17] J. Zhang, T. Darcie, and J. J. Eun, "High-performance passive microwave-photonic link for antenna remoting using truncated single-sideband optical phase detection," in *OFC/NFOEC, Anaheim, CA, 2007*, Paper OWU4.
- [18] P. Driessen, T. Darcie, and J. Zhang, "Analysis of a class-B microwave-photonic link using optical frequency modulation," *J. Lightw. Technol.*, vol. 26, no. 15, pp. 2740–2747, Aug. 1, 2008.
- [19] X. Xie, J. Khurgin, J. Kang, and F.-S. Choa, "Ring-assisted frequency discriminator with improved linearity," *IEEE Photon. Technol. Lett.*, vol. 14, no. 8, pp. 1136–1138, Aug. 2002.
- [20] G. Chen, J. Kang, and J. Khurgin, "Frequency discriminator based on ring-assisted fiber Sagnac filter," *IEEE Photon. Technol. Lett.*, vol. 17, no. 1, pp. 109–111, Jan. 2005.
- [21] J. Capmany, B. Ortega, and D. Pastor, "A tutorial on microwave photonic filters," *J. Lightw. Technol.*, vol. 24, no. 1, pp. 201–229, Jan. 2006.
- [22] C. K. Madsen and J. H. Zhao, *Optical Filter Design and Analysis*. New York: Wiley, Jun. 1999.
- [23] V. Urick, F. Bucholtz, P. Devgan, J. McKinney, and K. Williams, "Phase modulation with interferometric detection as an alternative to intensity modulation with direct detection for analog-photonic links," *IEEE Trans. Microw. Theory Tech.*, vol. 55, no. 9, pp. 1978–1985, Sep. 2007.
- [24] B. E. Little, S. T. Chu, P. P. Absil, J. V. Hryniewicz, F. G. Johnson, F. Seiferth, D. Gill, V. Van, O. King, and M. Trakalo, "Very high-order microring resonator filters for WDM applications," *IEEE Photon. Technol. Lett.*, vol. 16, no. 10, pp. 2263–2265, Oct. 2004.
- [25] B. Moslehi, J. Goodman, M. Tur, and H. Shaw, "Fiber-optic lattice signal processing," *Proc. IEEE*, vol. 72, no. 7, pp. 909–930, Jul. 1984.
- [26] B. Kumar and S. Dutta Roy, "Design of digital differentiators for low frequencies," *Proc. IEEE*, vol. 76, no. 3, pp. 287–289, Mar. 1988.
- [27] B. Kumar and S. C. D. Roy, "Maximally linear FIR digital differentiators for midband frequencies," *Int. J. Circuit Theory Appl.*, vol. 17, no. 1, pp. 21–27, Nov. 1989.
- [28] B. Kumar, S. Roy, and H. Shah, "On the design of FIR digital differentiators which are maximally linear at the frequency π/p , $p \in \{\text{positive integers}\}$," *IEEE Trans. Signal Process.*, vol. 40, no. 9, pp. 2334–2338, Sep. 1992.
- [29] D. Tishinin, P. Dapkus, A. Bond, I. Kim, C. Lin, and J. O'Brien, "Vertical resonant couplers with precise coupling efficiency control fabricated by wafer bonding," *IEEE Photon. Technol. Lett.*, vol. 11, no. 8, pp. 1003–1005, Aug. 1999.
- [30] M. Bohn, W. Rosenkranz, F. Horst, B. J. Offrein, G. L. Bona, and P. Krummrich, "Integrated optical FIR-filters for adaptive equalization of fiber channel impairments at 40 Gbit/s," in *Optical Communication Theory and Techniques*. Berlin, Germany: Springer, 2005, pp. 181–187.



John M. Wyrwas (S'06) received the B.S. degrees in physics and electrical engineering from the University of Maryland, College Park, in 2007 and is currently pursuing the Ph.D. degree in electrical engineering and computer science at the University of California, Berkeley.

His research interests are the area of high-speed optoelectronics including optical injection locking of semiconductor lasers, silicon integrated photonics, microwave photonics, optoelectronic oscillators and optical communications.



Ming C. Wu (S'82–M'83–SM'00–F'02) received the B.S. degree in electrical engineering from National Taiwan University, Taipei, Taiwan, and the M.S. and Ph.D. degrees in electrical engineering and computer sciences from the University of California, Berkeley, in 1985 and 1988, respectively.

From 1988 to 1992, he was a Member of Technical Staff at AT&T Bell Laboratories, Murray Hill, NJ. From 1992 to 2004, he was a Professor in the electrical engineering department at the University of California, Los Angeles, where he also served as Vice

Chair for Industrial Affiliate Program and Director of Nanoelectronics Research Facility. In 2004, he moved to the University of California, Berkeley, where he is currently Professor of electrical engineering and computer sciences. He is also a Co-Director of Berkeley Sensor and Actuator Center (BSAC). His research interests include Optical MEMS (micro-electro-mechanical systems), high-speed semiconductor optoelectronics, nanophotonics, and biophotonics. He has published six book chapters, over 135 journal papers and 280 conference papers. He is the holder of 14 U.S. patents.

Prof. Wu is a Fellow of IEEE, and a member of Optical Society of America. He was a Packard Foundation Fellow from 1992 to 1997. He is the founding Co-Chair of IEEE/LEOS Summer Topical Meeting on Optical MEMS (1996), the predecessor of IEEE/LEOS International Conference on Optical MEMS. He has served in the program committees of many technical conferences, including MEMS, OFC, CLEO, LEOS, MWP, IEDM, DRC, ISSCC; and as Guest Editor of two special issues of IEEE journals on Optical MEMS.